

Exact solution of the minimalist Stark many-body localization problem in terms of spin-pair hopping

Alexander L. Burin

Tulane University, New Orleans, Louisiana 70118, USA



(Received 27 October 2021; revised 18 May 2022; accepted 19 May 2022; published 31 May 2022)

Simultaneous conservation of charge (spin projection to the z axis) and dipole moment can partially suppress ergodicity (thermalization) by means of shattering the phase space. This shattering results in many-body localization of some states even in the absence of disordering, while other states remain delocalized. Here we show for the minimalist one-dimensional spin- $\frac{1}{2}$ model how to distinguish localized and delocalized states, based on any representative product state with given projections of spins to the z axis, separating states into four groups characterized by distinguishable behaviors. These include two groups of delocalized states with translationally invariant Krylov subspaces with integrable (group I) or ergodic (group II) dynamics, and the other two groups with confined spin transport having either all mobile spins (group III) or some immobile (frozen) spins (group IV). The states of the first two groups are delocalized, while the states of the last two groups are mostly localized. The theory is used to interpret recent experiments [Q. Guo *et al.*, *Phys. Rev. Lett.* **127**, 240502 (2021); W. Morong *et al.*, *Nature (London)* **599**, 393 (2021)], and suggests their extension necessary to observe both localized and delocalized behaviors in a dipole moment conserving regime.

DOI: [10.1103/PhysRevB.105.184206](https://doi.org/10.1103/PhysRevB.105.184206)

I. INTRODUCTION

Ergodicity breakdown represents the failure of quantum statistical mechanics [1–3] and gives advantages for quantum information processing in many-body systems [4–6]. It takes place in the form of many-body localization (MBL) due to strong disordering [7–10] similarly to the single-particle Anderson localization [11,12] or can be possibly realized without disordering [3,13–31]. Localization without disorder is an exciting fundamental task since it conflicts with the common sense expectations. It is also an attractive experimental challenge for researchers in a quantum information area [32,33] because of the localization robustness. Indeed, the localization in a regular system is insensitive to a specific disorder realization.

Disorder-free localization was considered at high temperature due to thermal disorder in positions of interacting particles [13]. It emerges in a thermodynamic limit of infinite system if some particles are static [27,28]; yet it is unstable with respect to arbitrary small deviation from a static behavior [3,34]. However, the localization can be robust in systems conserving not only number of particles, but the dipole moment or higher moments [35–47]. Dipole moment is approximately conserved in fractional quantum Hall effect [36,48–50] and systems subjected to a large potential energy gradient compared to the bandwidth (Stark MBL, Refs. [29–31,51]). On the one hand some eigenstates in those systems are completely *frozen*, i.e., they are characterized by fixed spin projections to the z axis [35], while on the other hand there exist other fully delocalized ergodic eigenstates [36,37,41,52]. Eigenstate behavior (localized or delocalized) in systems with local, dipole moment conserving hopping [35–38,41] depends on any representative product

state determining the unique Krylov subspace of all product states coupled to that state by the system Hamiltonian. It was demonstrated that different families of Krylov subspaces exist with different dynamical properties, including localizing and nonlocalizing dynamics. *These findings [35–38,41] motivate us to seek for the determination of eigenstate properties using their representative product states, which is the primary target of this work.*

The product states are usually chosen in the experiments as the initial states [32,33,51] giving us the opportunity to realize any regime of interest by choosing the proper initial state. However, the full localization was reported in the dipole moment conserving regime of a large field gradient [32,33] independent of the initial state. Our second target is *to interpret these observations and suggest ways to attain the full diversity of behaviors.*

In this work we establish the unique connection between the basis product states and the localization of eigenstates in the minimalist, dipole moment conserving periodic model (the MM model) on a chain defined as (cf. Refs. [36,37,51,53])

$$\hat{H}_{\text{MM}} = \Delta \sum_{k=1}^N (S_k^+ S_{k+1,p}^- S_{k+2,p}^- S_{k+3,p}^+ + \text{H.c.}) + 2\Delta \sum_{k=1}^N S_k^z (S_{k+1,p}^z - S_{k+2,p}^z), \quad (1)$$

where $S_{k,p}^a = S_k^a$ for $k \leq N$ and $S_{k,p}^a = S_{k-N}^a$ for $k > N$ ($a = +, -$ or z). The dipole moment $\hat{P} = \sum_{k=1}^N S_k^z (k - (N+1)/2)$ is conserved in this model with the accuracy to an integer number of N 's (modulo N) [41].

The present model is defined as the outcome of the parent XY model with the nearest- and next-neighbor interactions subjected to the large field gradient that is approximately relevant to the systems investigated in Refs. [32,33]. In Sec. II we show that the periodicity in space in Eq. (1) can be attained applying transverse (XY model) and longitudinal (Stark field) interactions consecutively and periodically in time. Equation (1) is derived using the generalized Schrieffer-Wolff transformation [54–58], in the lowest nonvanishing order in inverse field gradient F . The violation of spatial periodicity of the parent model results in additional longitudinal fields emerging in the lower order in F . These fields function as quenched disorder causing the localization of all states at sufficiently large field gradient observed experimentally [32,33] as discussed in Sec. IV.

In Sec. III we investigate the Krylov subspaces of product spin states of the model (1) and introduce the four groups of states distinguished by their dynamic behavior as confirmed by the analysis of group-averaged imbalances. In Sec. IV the experimental data of Refs. [32,33] are discussed in light of our findings. The work ends by the extended conclusion and discussion Sec. V, where the results of this work are briefly resumed, the comparison of them with the earlier work is outlined, and the generalization to other models is discussed. The long derivations are placed in the Supplemental Material [59].

II. PARENT MODEL AND DERIVATION OF MINIMALIST MODEL

The analytical results of this work are mostly related to the minimalist periodic dipole moment conserving model, given by Eq. (1). This model represents the first nonvanishing expansion term of the generalized Schrieffer-Wolff transformation [54–58] of the parent XY model subjected to the uniformly growing field in the large field gradient limit. Below we derive the Hamiltonian (1) for both open and periodic boundary conditions (OBC and PBC). The former case describes the experiments [32,33], while the latter case represents their desirable generalization that realizes a spatial periodicity insensitive to boundaries, which are dramatically important for the delocalization in a large field gradient limit (see Sec. IV). The derivation below is not related to dynamic properties of the model (1) considered in Sec. III so those readers, who are interested only in the analysis of this model, can skip it.

The minimalist model (MM) in Eq. (1) differs from the model of Refs. [37,41] referred here as the minimalist hopping only (MH) model by the presence of the longitudinal term containing S^z operators. As it is shown in the present section this term necessarily emerges as the outcome of the Schrieffer-Wolff transformation of the parent XY model subjected to the strong field gradient. Longitudinal and transverse interactions are of the same order of magnitude.

The other parent models including that of the fractional quantum Hall effect in the thin-torus limit [36,48–50] or the anisotropic Heisenberg model with nearest-neighbor interactions subjected to a large field gradient [41,60,61] also lead to a significant longitudinal interactions within the effective Hamiltonian in addition to the MH model Hamiltonian

of Refs. [37,41]. In those models, longitudinal interactions exceed the transverse ones in contrast with Eq. (1), where longitudinal and transverse interactions are comparable. Longitudinal interaction does not modify Krylov subspaces of relevant product states. However, it affects spin dynamics in those states, as discussed in Sec. VB, enhancing the localization.

A. Effective Hamiltonian of dipole moment conserving system with open boundary conditions

We begin with the derivation of the effective Hamiltonian for the general XY model with open boundary conditions subjected to a field uniformly increasing by a certain gradient F between adjacent sites. This model can be characterized by the Hamiltonian \hat{H} expressed as the sum of the field (\hat{H}_F) and XY model (\hat{H}_{XY}) Hamiltonians:

$$\hat{H} = \hat{H}_F + \hat{H}_{XY}, \quad \hat{H}_F = -F \sum_{k=1}^N \left(k - \frac{N+1}{2} \right) S_k^z, \\ \hat{H}_{XY} = \frac{1}{2} \sum_{i<j}^N J_{ij} (S_i^+ S_j^- + S_j^- S_i^+). \quad (2)$$

This model, referred as the parent OBC model, characterizes both transmon qubits within the superconducting quantum processor, investigated in Ref. [32], where the interaction is limited to nearest and next neighbors, and pseudospin states of interacting $^{171}\text{Yb}^+$ ions, investigated in Ref. [33], where the interaction depends on the distance as $J_{ij} = J/|i-j|^{1.3}$. The minimalist model (1) is the outcome of the Schrieffer-Wolff transformation of the parent model (2) in the large field gradient limit $F > J_{ij}$ with the only nearest- and next-neighbor interactions (J_1 and J_2 , respectively) different from zero. The minimalist XY model relevant for the many-body localization problem cannot be restricted to only nearest-neighbor interactions because this model is equivalent to noninteracting fermions [62].

In a large field gradient limit $F \gg J$ the effective Hamiltonian projected to the subspace of states with identical dipole moments can be derived using the Schrieffer-Wolff transformation similarly to Refs. [37,57]. The zeroth-order Hamiltonian is the longitudinal field Hamiltonian \hat{H}_F and the perturbation is given by the XY model Hamiltonian \hat{H}_{XY} in Eq. (2). Since any term in the perturbation does not conserve the dipole moment and thus modifies the zeroth-order energy by a large field gradient F the Schrieffer-Wolff transformation is well justified at large field gradients $F \gg J_{ij}$.

Applying the Schrieffer-Wolff transformation we modify the original Hamiltonian as

$$\hat{H} \rightarrow e^{\hat{S}} \hat{H} e^{-\hat{S}}, \quad (3)$$

where \hat{S} is an anti-Hermitian matrix chosen to eliminate the perturbation Hamiltonian \hat{H}_{XY} in the first order in \hat{S} that requires $[\hat{S}, \hat{H}_F] = -\hat{H}_{XY}$. This is sufficient to derive the effective Hamiltonian in a desirable third order, where the minimalist model (1) emerges.

The matrix \widehat{S} is defined in terms of raising and lowering spin operators $S_k^\pm = S_k^x \pm iS_k^y$ as

$$\widehat{S} = \frac{1}{2} \sum_{i < j}^N \frac{J_{ij}}{F(j-i)} (S_i^+ S_j^- - S_j^- S_i^+). \quad (4)$$

The expansion of the effective Hamiltonian (3) in \widehat{S} up to the third-order term yields [63]

$$\widehat{H} \approx \widehat{H}_F + \left\{ \frac{1}{2} [\widehat{S}, \widehat{V}] + \frac{1}{3} [\widehat{S}, [\widehat{S}, \widehat{V}]] \right\}_P, \quad (5)$$

where the subscript P in the definition of the effective Hamiltonian \widehat{H}_{eff} means that the only terms conserving dipole moment P (modulo N) are left. The third-order term is left together with the second-order one since the spin-spin interaction in the XY model appears only in the third order in \widehat{V} [57,58].

The second-order term can be expressed as [57]

$$\widehat{H}_2 = \frac{1}{2} [\widehat{S}, \widehat{V}] = \frac{1}{4F} \sum_i S_i^z \sum_{j \neq i} \frac{J_{ij}^2}{(i-j)}. \quad (6)$$

Equation (6) introduces a site-dependent longitudinal field acting on each spin. For the interaction determined by the interspin distance only, i.e., $J_{ij} = J(|i-j|)$ this term disappears in the macroscopic limit of an infinite number of spins because the sum over j is antisymmetric. This is the case for the cold ions considered in Ref. [33] in the limit $N \rightarrow \infty$, while the interaction of transmon qubits in Ref. [32] does not satisfy the rule $J_{ij} = J(|i-j|)$ since it vanishes for certain pairs of next-neighbor spins.

The interaction (6) is significant for both experiments [32,33] under consideration and it is responsible for the localization observed experimentally at different initial states for large field gradients as shown in Sec. V below. However, this second-order term disappears in periodic settings as shown in Sec. II B. Therefore, it is ignored in Eq. (1) where the periodic model is considered.

The transverse hopping interaction violating the dipole moment conservation also emerges in the second order in JF^{-1} in the form

$$\widehat{H}_{2,\text{offd}} = \frac{1}{16F} \sum_{j \neq l, k} \frac{(j+l-2k)J_{jk}J_{kl}S_k^z S_j^+ S_l^-}{(j-k)(l-k)}. \quad (7)$$

An additional Schrieffer-Wolff transformation is needed to eliminate it. This transformation will generate dipole moment conserving interactions of order of $J^4 F^{-3}$, which is smaller in the large field gradient limit compared to the interactions described by the second term in the expansion (5). This term contains both diagonal binary spin interaction [57] and transitions in spin quartets [58]. The diagonal interaction takes the form

$$\widehat{H}_{3d} = \frac{1}{2F^2} \sum_{j < k} S_j^z S_k^z \sum_l \frac{J_{jk}J_{kl}J_{lj}}{(k-l)(j-l)}. \quad (8)$$

If the hopping interaction is limited to nearest neighbors, i.e., the only interaction $J_{i,i+1} = J_1$ differs from zero, then all interactions in Eq. (8) are equal to zero [57] due to a single-particle nature of the XY model with nearest-neighbor interactions

[62]. In the minimalist XY model with nearest- and next-neighbor hopping interactions ($J_{i,i+1} = J_1, J_{i,i+2} = J_2$) Eq. (8) generates nearest- and next-neighbor interactions in the form $\sum_{i < j} U_{ij} S_i^z S_j^z$ with interaction constants U_{ij} defined as

$$U_{ij} = \frac{J_1^2 J_2}{4F^2} [\delta_{i,j-1}(2 - \delta_{i1} - \delta_{jN}) - \delta_{i,j-2}]. \quad (9)$$

Thus, the nearest- and next-neighbor longitudinal interactions $\pm \Delta$, respectively, with $\Delta = J_1^2 J_2 / (2F^2)$ are generated for all sites except for those at the edges [cf. Eq. (1)] where the nearest-neighbor interaction is smaller by the factor of 2.

The off-diagonal four-spin hopping interaction conserving dipole moment can be evaluated similarly to Ref. [58] as

$$\widehat{H}_{3,\text{offd}} = \sum_{i < j < k < l} V_{ijkl} \delta_{i+l, j+k} S_i^+ S_j^- S_k^- S_l^+, \quad (10)$$

where δ_{ab} is the Kronecker symbol and the four-spin interaction V_{ijkl} can be expressed as

$$J_{ijkl} = -\frac{1}{4F^2} \left(\frac{J_{ij}J_{ik}J_{il}}{(i-j)(i-k)} + \frac{J_{il}J_{jl}J_{kl}}{(l-j)(l-k)} \right. \\ \left. + \frac{J_{ij}J_{jk}J_{jl}}{(j-i)(j-k)} + \frac{J_{jk}J_{kl}J_{kl}}{(k-i)(k-l)} \right). \quad (11)$$

If the only nearest-neighbor interaction $J_{i,i+1} = J_1$ differs from zero the four-spin hopping amplitude disappears [58] that is the consequence of a single-particle nature of XY model with nearest-neighbor interactions [62]. For the simplest many-body XY model with nonzero nearest- and next-neighbor interactions ($J_{i,i+1} = J_1, J_{i,i+2} = J_2$), Eq. (11) leads to a nonzero hopping for only consecutive spin quartets $i, i+1, i+2, i+3$. For those quarters the only two last terms in Eq. (11) contribute to the four-spin hopping amplitude $\Delta = J_{i,i+1,i+2,i+3} = J_1^2 J_2 / (4F^2)$ [cf. Eq. (1)].

B. Case of periodic boundary conditions.

Here we derive the effective Hamiltonian (1) for the periodic model with a finite number of spins that is the main subject of study for this work. We suggest the realization of the fully periodic Stark MBL problem for a finite number of spins insensitive to the boundary conditions that can be realized experimentally.

To make hopping periodic within the experimental settings of Refs. [32,33] one should connect transmon qubits used in Ref. [32] periodically or place cold ions investigated in Ref. [33] equidistantly in a circle. This should make spin-hopping amplitudes in Eq. (2) periodic, i.e., $J_{ij} = J_{i+N,j} = J_{i,j+N}$. A uniformly increasing field can be made periodic on a circle using time-periodic Hamiltonian defined as [cf. Eq. (2)]

$$\widehat{H}(t) = \begin{cases} \widehat{H}_F & \text{for } 2k\tau_F < t < (2k+1)\tau_F, \\ \widehat{H}_{XY} & \text{for } (2k+1)\tau_F < t < 2(k+2)\tau_F, \end{cases} \\ \tau_F = \frac{2\pi}{NF}, \quad k = 0, \pm 1, \pm 2, \dots \quad (12)$$

The time period $2\tau_F$ is chosen to make the interaction associated with the field gradient F periodic on a circle. This periodicity can be understood considering the system evolution matrix describing the Hamiltonian (12) action during a

period as

$$\begin{aligned}\widehat{U} &= \widehat{U}_{ph}\widehat{U}_{XY}, \quad \widehat{U}_{ph} = e^{-i\sum_{k=1}^N \frac{2\pi k}{N} S_k^z} = e^{-i\widehat{S}_0}, \\ \widehat{U}_{XY} &= e^{-\sum_{k \neq j} \frac{2\pi i k_j}{NF} S_k^+ S_j^-} = e^{-i\widehat{S}_1}.\end{aligned}\quad (13)$$

In a large field gradient limit this evolution matrix allows conservation of the dipole moment $P = \sum_{k=1}^N (k - \frac{N+1}{2}) S_k^z$ with the accuracy to the integer number of spin numbers N since the change of the dipole moment by N modifies the evolution matrix \widehat{U}_{ph} by $e^{2\pi i} = 1$. This is exactly the change of the dipole moment by N in the four-spin hopping involving edges (e.g., $S_{N-2}^- S_{N-1}^+ S_N^+ S_1^-$) that makes this hopping periodic on a circle [41]. The periodicity on a circle of the effective Hamiltonian conserving dipole moment emerges naturally during its construction as derived below.

To be more specific, we define periodicity on a circle for a certain operator as following. For any multispin interactions within this operator that can be generally expressed as $J_{i_1, i_2, \dots, i_n}^{\alpha_1, \alpha_2, \dots, \alpha_n} S_{i_1}^{\alpha_1} S_{i_2}^{\alpha_2} \dots S_{i_n}^{\alpha_n}$ ($\alpha_i = \pm, z$) the conditions of translational invariance and periodicity on a circle must be satisfied. These conditions can be written as (respectively)

$$\begin{aligned}J_{i_1+a, i_2+a, \dots, i_n+a}^{\alpha_1, \alpha_2, \dots, \alpha_n} &= J_{i_1, i_2, \dots, i_n}^{\alpha_1, \alpha_2, \dots, \alpha_n}, \quad a = 1, 2, 3, \dots \\ J_{i_1, i_2, \dots, i_k+N, \dots, i_n}^{\alpha_1, \alpha_2, \dots, \alpha_n} &= J_{i_1, i_2, \dots, i_k, \dots, i_n}^{\alpha_1, \alpha_2, \dots, \alpha_n}, \quad 1 \leq k \leq N.\end{aligned}\quad (14)$$

The effective Hamiltonian derived by means of the generalized Schrieffer-Wolff transformation (15) possesses the property (14) as shown below in Sec. II B 1.

The period $2\tau_F$ of the Hamiltonian $\widehat{H}(t)$ [Eq. (12)] is the minimum time needed to make a finite system periodic. For this specific choice in the limit of a large field gradient F the approximate conservation of the dipole moment (modulo N) takes place as needed to support a periodic spin hopping (see Ref. [41]). The period chosen as any integer multiple of $2\tau_F$ ($2k\tau_F$ with an integer, nonzero k) also ensures the spatial periodicity. Yet, in that case the dipole moment is conserved with the accuracy to an addition of integer numbers of N/k . This can lead to appearance of more terms in the effective Hamiltonian conserving the dipole moment. For instance, if $k = 2$ and N is even the hopping terms like $S_k^+ S_{k+N/2}^-$ modifying the system dipole moment by $N/2$ will be also allowed. Additional hopping can reduce the localization contrary to the original goal to attain it in the maximum extent. Therefore, we use the minimum possible period $2\tau_F$.

1. Transformation of the evolution matrix

To eliminate off-resonant processes and create the effective Hamiltonian conserving quasidipole moment P (modulo N) or $e^{2\pi i \sum_{k=1}^N [k - (N+1)/2] S_k^z / N}$ [41], one can apply a generalized Schrieffer-Wolff transformation [63] to the evolution matrix (13) for a period in the form

$$\tilde{U}_* = e^{\widehat{S}} \widehat{U} e^{-\widehat{S}} \quad (15)$$

with the anti-Hermitian matrix \widehat{S} (wave functions should be modified simultaneously as $\psi \rightarrow e^{\widehat{S}} \psi$).

The goal of the transformation is to bring the evolution matrix to the form

$$\widehat{U}_* = \widehat{U}_{ph} e^{-i\widehat{H}_{\text{eff}} \tau_F}, \quad (16)$$

with the effective Hamiltonian \widehat{H}_{eff} conserving the dipole moment (modulo N). This goal can be approximately attained eliminating the leading (in JF^{-1}) interactions modifying dipole moment in the system Hamiltonian using the generalized Schrieffer-Wolff transformation. Then, the Baker-Campbell-Hausdorff-Dynkin formula [55,56] should be applied to express the action of modified evolution matrices in terms of a single effective Hamiltonian \widehat{H}_{eff} . This new iteration for the effective Hamiltonian will have interactions violating the dipole moment conservation smaller by a factor of J/F compared to the original Hamiltonian similarly to the standard Schrieffer-Wolff transformation [63] as illustrated below in Sec. II B 2. This procedure should be repeated an infinite number of times to get rid of the off-resonant interaction in all orders in JF^{-1} . It should converge at large field gradients F [64] as confirmed by our numerical calculations reported below in Sec. IV.

We expect that the effective Hamiltonian in Eq. (16) is periodic on a circle as defined by Eq. (14). To show that one can represent the transformed evolution matrix introducing the operator \widehat{S}_{mod} as

$$\begin{aligned}\tilde{U}_* &= e^{\widehat{S}} \widehat{U}_{ph} \widehat{U}_{XY} e^{-\widehat{S}} = \widehat{U}_{ph} e^{\widehat{S}_{\text{mod}}} \widehat{U}_{XY} e^{-\widehat{S}}, \\ \widehat{S}_{\text{mod}} &= \widehat{U}_{ph}^{-1} \widehat{S} \widehat{U}_{ph}.\end{aligned}\quad (17)$$

The Hamiltonian \widehat{H}_{XY} and the associated evolution matrix \widehat{U}_{XY} are periodic on a circle. Assume that this is true for the operator \widehat{S} and this operator also conserves the projection of spin to the z axis as the original Hamiltonian. The latter is obviously true for the standard Schrieffer-Wolff transformation.

Then the same is true for the operator \widehat{S}_{mod} . Indeed, if the operator \widehat{S} depends on operators $\{S_n^\alpha\}$ ($\alpha = \pm, z$, $n = 1, 2, \dots, N$) then the operator \widehat{S}_{mod} is the identical function of those operators, modified as $S_n^\pm \rightarrow S_n^\pm e^{\pm 2\pi i n / N}$, $S_n^z \rightarrow S_n^z$. For the modified operator the property of translational invariance [the first line in Eq. (14)] is valid because of the identical number of S^+ and S^- operators in each term as required by the spin projection conservation. Therefore, the additional factors $e^{\pm 2\pi i a / N}$ [where a is the shift of indices in Eq. (14)] compensate each other. The periodicity with the period N is satisfied since the addition of the number of spins N to the spin position n in the exponents $e^{\pm 2\pi i n / N}$ accompanying operators S_n^\pm modifies them as $e^{\pm 2\pi i (n+N) / N}$ thus multiplying them by $e^{\pm 2\pi i} = 1$. The construction of the operator \widehat{S} is demonstrated below in Sec. II B 2.

2. Effective Hamiltonian in the leading (third) order of $1/F$ expansion

To find the effective Hamiltonian \widehat{H}_{eff} in the first non-vanishing order in J_{ij}/F one can use the transformation eliminating the interaction \widehat{S}_1 violating the dipole moment conservation and generating dipole moment conserving terms. To find such transformation we introduce an operator \widehat{S}_{mod} as [cf. Eq. (17)]

$$e^{\widehat{S}} e^{-i\widehat{S}_0} = e^{-i\widehat{S}_0} e^{\widehat{S}_{\text{mod}}}. \quad (18)$$

Then, the modified evolution matrix can be expressed in the form

$$\tilde{U} = e^{-i\hat{S}_0} e^{\hat{S}_{\text{mod}}} e^{-i\hat{S}_1} e^{-\hat{S}}. \quad (19)$$

The exponent $e^{-i\hat{S}_1}$ gets canceled in the first nonvanishing order in \hat{S}_1 if

$$\hat{S}_{\text{mod}} - i\hat{S}_1 - \hat{S} = 0. \quad (20)$$

Seeking the operator \hat{S} in the general form of the sum of binary products of spin-raising and -lowering operators

$$\hat{S} = \sum_{k,l} A_{kl} S_k^+ S_l^- \quad (21)$$

one can express the modified exponent as

$$\hat{S}_{\text{mod}} = \sum_{k,l} A_{kl} S_k^+ S_l^- e^{2\pi i \frac{k-l}{N}}. \quad (22)$$

$$\begin{aligned} \hat{H}_{\text{eff}} &= [\hat{H}_*]_P, \quad \hat{H}_* = \frac{1}{i\tau_F} (-\hat{S}_{\text{mod}} + i\hat{S}_1 + \hat{S}) + \frac{i}{2i\tau_F} (i[\hat{S}_{\text{mod}}, \hat{S}_1] + [\hat{S}_{\text{mod}}, \hat{S}] - i[\hat{S}_1, \hat{S}]) \\ &+ \frac{i}{12\tau_F} (-i[\hat{S}_{\text{mod}}, [\hat{S}_{\text{mod}}, \hat{S}_1]] + [\hat{S}_1, [\hat{S}_{\text{mod}}, \hat{S}_1]] - 3i[\hat{S}, [\hat{S}_{\text{mod}}, \hat{S}_1]]) \\ &+ \frac{i}{12\tau_F} (-i[\hat{S}_{\text{mod}} - i\hat{S}_1, [\hat{S}_{\text{mod}} - i\hat{S}_1, \hat{S}]] - [\hat{S}, [\hat{S}_{\text{mod}} - i\hat{S}_1, \hat{S}]]) \end{aligned} \quad (25)$$

where the subscript P in the definition of the effective Hamiltonian \hat{H}_{eff} means that the only terms conserving dipole moment P (modulo N) are left. Using Eq. (20) one can simplify the Hamiltonian expressing it in terms of \hat{S}_{mod} and \hat{S} operators as (particularly, the first term and the last line vanish because $\hat{S}_{\text{mod}} - i\hat{S}_1 = -\hat{S}$)

$$\begin{aligned} \hat{H}_* &= \frac{i}{2\tau_F} [\hat{S}_{\text{mod}}, \hat{S}] + \frac{i}{6\tau_F} ([\hat{S}_{\text{mod}}, [\hat{S}_{\text{mod}}, \hat{S}]] \\ &+ [\hat{S}, [\hat{S}_{\text{mod}}, \hat{S}]]) \end{aligned} \quad (26)$$

Consider the second-order term [the first term in Eq. (26), which is of the second order in J/F compared to the leading Stark term, that is proportional to F]. This term being projected to the subspaces of the Hilbert space with identical dipole moments is represented by spin-dependent longitudinal fields that can be expressed as [cf. Eq. (6)]

$$\hat{H}_2 = -\frac{\pi}{4NF} \sum_{j,k} J_{kj}^2 \cot[\pi(k-j)/N] S_k^z. \quad (27)$$

If the interaction J_{ij} is periodic on a circle Eq. (14), this term vanishes because the sum over j is antisymmetric. This is the significant advantage of the periodic (PBC) model compared to its OBC counterpart, where this second-order term dramatically suppresses the delocalization creating effective disorder (see Sec. V).

The transverse term emerging in the same order in J_{ij}/F does not conserve the dipole moment and can be neglected similarly to the analogous term for the OBC problem (7), when considering the contributions to the effective

The amplitudes A_{kl} satisfying Eq. (20) are defined as

$$A_{kl} = -\frac{1}{2NF} \frac{2\pi i J_{kl}}{1 - e^{2\pi i \frac{k-l}{N}}}. \quad (23)$$

This definition of the amplitudes A_{kl} satisfies the requirement $A_{lk} = -A_{kl}^*$ so the transformation of the evolution matrix in Eq. (15) is unitary as it is supposed to be. In the limit of large N the operator \hat{S} becomes fully identical to the operator corresponding to the Schrieffer-Wolff transformation in Eq. (4) for open boundary conditions.

Using this definition of the transformation one can represent the evolution matrix (15) in the form of Eq. (16) as

$$\tilde{U} \approx e^{-i\hat{S}_0} e^{-i\hat{H}_{\text{eff}}\tau_F}, \quad (24)$$

with the effective Hamiltonian containing only resonant terms conserving dipole moment (modulo N). The effective Hamiltonian can be obtained using the Baker-Campbell-Hausdorff-Dynkin formula [56] up to the third order in JF^{-1} in the form

Hamiltonian up to the third order in JF^{-1} . However, it contributes to the fourth-order interactions discussed in Sec. II C.

The third-order (in JF^{-1}) dipole-moment conserving contributions to the effective Hamiltonian comes from longitudinal and transverse terms

$$\hat{H}_{\text{eff}} = \hat{H}_{3,l} + \hat{H}_{3,tr}. \quad (28)$$

The longitudinal term representing the induced longitudinal spin-spin interactions can be evaluated similarly to Ref. [57] and Eq. (8) as

$$\begin{aligned} \hat{H}_{3,l} &= \sum_{j < k} U_{jk} S_j^z S_k^z, \quad U_{jk} \\ &= \frac{\pi^2}{6N^2 F^2} \frac{J_{jk} J_l J_{kl} [2 \cos(\frac{\pi(j-k)}{N}) + \cos(\frac{\pi(2l-j-k)}{N})]}{\sin(\frac{\pi(l-j)}{N}) \sin(\frac{\pi(l-k)}{N})} \end{aligned} \quad (29)$$

The transverse part of the effective Hamiltonian (28) can be evaluated similarly to the OBC case of Eqs. (10) and (11) as

$$\begin{aligned} \hat{H}_{3,\text{offd}} &= \sum_{j,k,l,m} V_{jklm} S_j^+ S_k^- S_l^+ S_m^- \Delta_N(j+l-k-m), \\ \Delta_N(a) &= \sum_{p=-\infty}^{\infty} \delta_{a,pN}, \end{aligned} \quad (30)$$

where δ_{ab} is the Kronecker symbol. The interaction V_{ijkl} is defined as

$$\begin{aligned}
V_{ijkl} = & -\frac{\pi^2}{12N^2F^2} \left(\frac{J_{ij}J_{ik}J_{il} \left[2 \cos\left(\frac{\pi(i-j)}{N}\right) \cos\left(\frac{\pi(i-k)}{N}\right) + (-1)^{i+l-j-k} \cos\left(\frac{\pi(i-l)}{N}\right) \right]}{\sin\left(\frac{\pi(i-j)}{N}\right) \sin\left(\frac{\pi(i-k)}{N}\right)} \right. \\
& + \frac{J_{ij}J_{jk}J_{jl} \left[2 \cos\left(\frac{\pi(i-j)}{N}\right) \cos\left(\frac{\pi(j-l)}{N}\right) + (-1)^{i+l-j-k} \cos\left(\frac{\pi(j-k)}{N}\right) \right]}{\sin\left(\frac{\pi(j-i)}{N}\right) \sin\left(\frac{\pi(j-l)}{N}\right)} \\
& + \frac{J_{ik}J_{jk}J_{kl} \left[2 \cos\left(\frac{\pi(i-k)}{N}\right) \cos\left(\frac{\pi(k-l)}{N}\right) + (-1)^{i+l-j-k} \cos\left(\frac{\pi(j-k)}{N}\right) \right]}{\sin\left(\frac{\pi(k-i)}{N}\right) \sin\left(\frac{\pi(k-l)}{N}\right)} \\
& \left. + \frac{J_{il}J_{kl}J_{il} \left[2 \cos\left(\frac{\pi(l-j)}{N}\right) \cos\left(\frac{\pi(l-k)}{N}\right) + (-1)^{i+l-j-k} \cos\left(\frac{\pi(i-l)}{N}\right) \right]}{\sin\left(\frac{\pi(l-j)}{N}\right) \sin\left(\frac{\pi(l-k)}{N}\right)} \right). \quad (31)
\end{aligned}$$

For the parent XY model with nonzero nearest- and next-neighbor interactions the generated diagonal interaction has the slightly modified form compared to Eq. (9)

$$\begin{aligned}
U_{ij} &= 2\Delta(\delta_{i,j-1} - \delta_{i,j-2}), \quad i < j \\
\Delta &= \eta(N) \frac{J_1^2 J_2}{4F^2}, \quad \eta(N) = \pi^2 \frac{2 \cos\left(\frac{2\pi}{N}\right) + 1}{3N^2 \sin\left(\frac{\pi}{N}\right)^2}. \quad (32)
\end{aligned}$$

The same constant Δ determines the four-spin hopping amplitude in Eq. (30) for four consecutive neighboring spins, while it is zero for all other spin quartets. Since the factor $\eta(N)$ very quickly approaches unity with increasing N [for instance, $\eta(15) = 0.9563$ for the minimum number of spins studied experimentally in Ref. [33]] we ignore its difference from unity and consider the minimalist model in the form of Eq. (1).

The spatial periodicity can be realized similarly in any other system with large field gradient including, e.g., Ref. [51].

C. Relevance of the minimalist model

Since the minimalist model in Eq. (1) is derived as the expansion of the effective Hamiltonian in inverse field gradient F this model should be relevant at sufficient large field gradient $F > F_c$. Here we summarize the estimates of the crossover field gradient F_c , while the details are given in the Supplemental Material [59], Sec. I.

The relevance of the minimalist model can be examined conservatively requiring the weak modification of eigenstate energies or liberally requiring the weak change in observables. In this paper we consider an imbalance in the infinite-time limit as the observable characterizing the system dynamics (see Sec. III F). In the Supplemental Material [59] (Sec. I C) energy levels and imbalances were compared for the minimalist model and more accurate models. All comparisons are performed for the XY model in Eq. (12) with nearest- and next-neighbor interactions different from zero and identical similarly to the experimentally investigated system in Ref. [32]. We set both interactions equal to J .

The conservative estimate can be obtained considering the minimalist model as the zeroth-order Hamiltonian and the fourth-order correction to it as a perturbation. Then a typical perturbation matrix element scales as $V_4 \sim 2^{-N/2} J^4 / F^3$ [65], while the typical interlevel spacing of the minimalist model

scales as $\delta E \sim 2^{-N} J^3 / F^2$. Setting $V_4 \approx \delta E$ we end up with the desirable estimate that is consistent with that of the Supplemental Material [59] (Sec. I C)

$$F_{c1} \approx 0.25 \times 2^{N/2} J, \quad (33)$$

obtained comparing the exact diagonalization results for the minimalist model and its corrected version.

The liberal estimate can be derived requiring the Schrieffer-Wolff expansion to be generally converging. Since the expansion parameter of the effective Hamiltonian is J/F the liberal criterion reads as

$$F_{c2} \approx J. \quad (34)$$

Even the conservative estimate can be insufficient since an arbitrary small nonlocal interaction emerging in higher orders in F^{-1} can destroy shattering and, consequently, localization. Our numerical analysis of imbalance shows that it does not happen. Moreover, the analysis of imbalances reported in the Supplemental Material [59] (Sec. I C) shows that the condition (34) is nearly sufficient for the qualitative relevance of the imbalance behavior obtained in the minimalist model, while the quantitative relevance of this model for localized states requires Eq. (33) to be satisfied. The liberal estimate is relevant quantitatively for delocalized groups of states.

The present conclusions for the liberal criterion are based on the numerical analysis limited to relatively small numbers of spins $N \leq 16$. We hope that its predictions can be extended to larger sizes; yet this is the subject for more accurate theoretical or experimental verifications.

III. GROUPS OF STATES: LOCALIZATION AND DELOCALIZATION WITHIN THE MINIMALIST MODEL

A. Inverted representation and pair hopping

The spin hopping in the minimalist model is represented by simultaneous hopping of two neighboring spins in opposite directions as $\uparrow\downarrow\uparrow\leftrightarrow\downarrow\uparrow\downarrow$ in consecutive spin quartets with oppositely oriented middle and border spins. In this picture the spin hopping is hard to trace visually. However, it is made easier by inverting each second spin as $\uparrow\uparrow\downarrow\leftrightarrow\downarrow\downarrow\uparrow$. Then, the spin hopping is represented by the hopping of pairs of spins oriented identically.

The transition from the original model (1) to the inverted spin-chain representation can be performed rotating all even-numbered spins about the x axis by the angle π . The transformation unitary matrix for this rotation is given by $\hat{U} = \prod_{k=1}^{N/2} e^{i\pi S_{2k}^x}$. It does not change spin operators in odd-numbered sites modifying operators at even-numbered sites as $S_{2k}^x \rightarrow \hat{U} S_{2k}^x \hat{U}^{-1} = S_{2k}^x$, $S_{2k}^y \rightarrow \hat{U} S_{2k}^y \hat{U}^{-1} = -S_{2k}^y$, $S_{2k}^z \rightarrow \hat{U} S_{2k}^z \hat{U}^{-1} = -S_{2k}^z$. Consequently, S^+ and S^- operators are interchanged at even-numbered sites, i.e., $S_{2k}^+ \rightarrow S_{2k}^-$ and $S_{2k}^- \rightarrow S_{2k}^+$. This modifies the minimalist model Hamiltonian (1) as

$$\hat{H}_{\min} = \Delta \sum_{k=1}^N (S_k^+ S_{k+1,p}^+ S_{k+2,p}^- S_{k+3,p}^- + \text{H.c.}) - 2\Delta \sum_{k=1}^N S_k^z (S_{k+1,p}^z + S_{k+2,p}^z), \quad (35)$$

where $S_{k,p}^a = S_k^a$ for $k \leq N$ and $S_{k,p}^a = S_{k-N}^a$ for $k > N$ ($a = +, -$ or z). This transformation is applicable only to states containing an even number of spins considered below, while the generalization of the results to an odd number of spins is given later in Sec. III E.

Inverted chain representation makes spin hopping truly visible. Indeed, consider the inverted state A composed by two sequences of oppositely oriented adjacent spins containing odd numbers of spins $\uparrow\uparrow\uparrow\uparrow\downarrow\downarrow\downarrow\downarrow$. We will refer to such sequences as *odd* sequences, while sequences containing even numbers of spins are referred as *even* sequences. It is clear from this picture how spin pairs can propagate through the chain. For example, the rightmost upwards oriented pair of fourth and fifth spins can hop three times to the right reaching 10th and 11th positions (state B : $\uparrow\uparrow\uparrow\downarrow\downarrow\downarrow\downarrow\uparrow\uparrow\downarrow$), while the leftmost pair of downwards oriented spins (sixth and seventh spins) can hop to the left maximum two times reaching second and third positions (state C : $\uparrow\downarrow\downarrow\uparrow\uparrow\uparrow\downarrow\downarrow\downarrow$). These states A , B , and C for the original spin chain look like $\uparrow\downarrow\uparrow\downarrow\uparrow\downarrow\uparrow\downarrow\uparrow$, $\uparrow\downarrow\uparrow\downarrow\uparrow\downarrow\uparrow\downarrow\uparrow$, and $\uparrow\uparrow\downarrow\downarrow\uparrow\downarrow\uparrow\downarrow\uparrow$, respectively. It is much more difficult to establish the visual connection between the latter three states compared to these states for the inverted chain.

The inverted-chain representation permits us to characterize spin hopping using the parity of sequences of adjacent spins having identical orientations. Odd or even sequences are sequences containing odd or even number of identically oriented consecutive spins, respectively. For instance, the state $\uparrow\uparrow\uparrow\downarrow\downarrow\downarrow\downarrow\uparrow\uparrow\downarrow$ is composed by sequences of 3, 6, 2, and 1 spins. One can define it by the set of numbers $\{3, 6, 2, 1\}$ specifying that the first spin of the first sequence is located in the first position of the periodic chain and it is oriented upwards. Due to the periodicity of the chain the state $\uparrow\uparrow\downarrow\downarrow\downarrow\downarrow\uparrow\uparrow\downarrow$ is defined by the same set of numbers with the second spin of the first sequence located in the first position of the periodic chain and oriented upwards.

B. Classification of Krylov subspaces: Localized and delocalized groups of states

Product states coupled by spin pair hops form the basis for system eigenstates and this basis defines the Krylov subspace

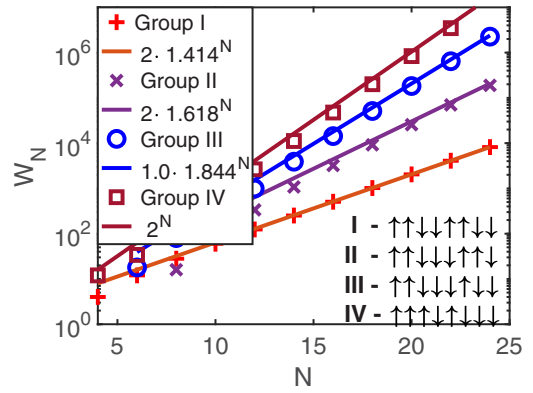


FIG. 1. Numbers of states vs the numbers of spins for all groups with representative states for all groups.

for a specific group of states [37,41]. The basis *product* states of an *inverted* chain can be represented as the set of consecutive numbers of identically oriented spins $\{n_1, n_2, \dots, n_p\}$ [e.g., $\{2, 3, 4, 3\}$ for the state A in Eq. (36)]. If sequences 1 and p are oriented identically, then they should be considered jointly as $\{n_1 + n_p, n_2, \dots, n_{p-1}\}$ with the specified position of the first spin. Pair hopping conserves the number of odd sequences since it can modify the sequence size only by 2. Therefore, the numbers of odd sequences are identical in all product states belonging to the given Krylov subspace, serving conserved quantities (cf. Ref. [38]).

The main results of this work can be formulated in terms of the relative parities of sequences shared between all product states belonging to the given Krylov subspace as following. If all odd- or even-numbered sequences are even (except for frozen states possessing all identical spins or having a single spin in all even- or odd-numbered sequences), then corresponding Krylov subspaces and system eigenstates possess the translational invariance with the period 2 [see, e.g., states in Eq. (36)]. Consequently, these states are delocalized. The remaining product states having odd sequences at both odd and even positions form Krylov subspaces (with marginal exceptions) with no translational invariance and confined spin transport.

Product states corresponding to translationally invariant Krylov subspaces can be separated into two groups of states enumerated by the roman numbers I and II. The group I consists of $2 \times 2^{N/2}$ states composed by all even sequences. The group I states can be mapped to $N/2$ spins $\frac{1}{2}$ representing pairs [48] (spin subspaces of Refs. [37,41]).

The states of the group II are formed by the product states possessing at least one odd sequence and all even sequences of spins oriented either upwards or downwards as in Eq. (36). Correspondingly, the odd sequences must have the opposite orientation. The number of states belonging to this group II behaves as $W_N \approx 2 \times [(1 + \sqrt{5})/2]^N \propto 1.618^N$ at large N . The numbers of states are calculated for all groups in the Supplemental Material [59] (Sec. II) using the generating function method, and presented in Fig. 1 together with the representative group states. All sectors of the Hilbert space spanned by states lying in group I correspond to integrable models [41], while the group II states are mostly ergodic as pointed out below in Sec. III C.

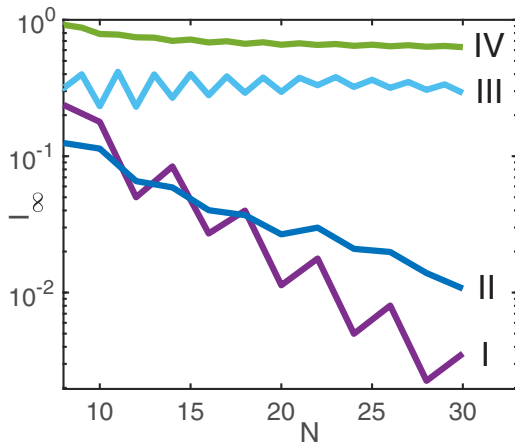


FIG. 2. Dependence of average imbalances evaluated within the infinite-time limit on the number of spins for different groups (solid lines with the group numbers in the right).

The states of both groups must have even numbers of spins. The original (noninverted) states are characterized by a zero-spin projection to the z axis. The zero-spin projection corresponds to the filling factor $\frac{1}{2}$ leading to at least twofold degeneracy of all states [49], which is realized for eigenstates of the problem (1) shifted by the one lattice period with respect to each other since they cannot be coupled by pair hopping.

The remaining nontranslationally invariant states can be represented by states containing at least two odd sequences with oppositely oriented spins. We separate them into two groups including the group III of states having no frozen spins, with conserved projections to the z axis, and group IV of states containing frozen spins as defined in Eq. (37) (for example, third, fourth, and fifth spins are frozen in the representative state of the group IV in Fig. 1). The group IV contains the majority of states ($\propto 2^N$). Localization obviously takes place for the group IV states split into independent blocks by frozen spins. The group III states are mostly localized for the present model (1) in accord with the imbalance behavior (see Fig. 2).

The states with odd number of spins belong either to the group III or IV depending on the presence of frozen spins [Eq. (37)] (see Sec. III E).

C. Translational invariance

Here we prove the translational invariance for the groups I and II and its absence for almost all Krylov's subspaces in groups III and IV. To prove the translational invariance for the groups I or II consider the product state belonging to these groups with even number of spins in all odd-numbered sequences. Such state is illustrated by the state $A = \{2, 3, 4, 3\}$ defined below as

$$\begin{array}{l}
 \begin{array}{cccccccccccc} 1 & 2 & 3 & 4 & 5 & 6 & 7 & 8 & 9 & 10 & 11 & 12 \\ \uparrow & \uparrow & \downarrow & \downarrow & \uparrow & \uparrow & \uparrow & \uparrow & \downarrow & \downarrow & \uparrow & \uparrow \end{array} \rightarrow \begin{array}{cccccccccccc} 1 & 2 & 3 & 4 & 5 & 6 & 7 & 10 & 11 & 8 & 9 & 12 \\ \uparrow & \uparrow & \downarrow & \downarrow & \uparrow & \uparrow & \downarrow & \downarrow & \uparrow & \uparrow & \uparrow & \downarrow \end{array} \\
 \begin{array}{cccccccccccc} 1 & 2 & 3 & 4 & 5 & 10 & 11 & 6 & 7 & 8 & 9 & 12 \\ \uparrow & \uparrow & \downarrow & \downarrow & \uparrow & \uparrow & \uparrow & \downarrow & \downarrow & \uparrow & \uparrow \end{array} \rightarrow \begin{array}{cccccccccccc} 3 & 4 & 1 & 2 & 5 & 10 & 11 & 6 & 7 & 8 & 9 & 12 \\ \downarrow & \downarrow & \uparrow & \uparrow & \downarrow & \downarrow & \uparrow & \uparrow & \uparrow & \uparrow & \uparrow \end{array}
 \end{array} \quad (36)$$

The translational invariance with the period 2 for these states can be demonstrated considering spin-pair hopping starting with the rightmost sequence k in even numbered position having more than one spin ($n_k > 1$) [spins 10, 11, 12 in the state A in Eq. (36)]. If there is only one spin there then another even-numbered sequence k should be considered with $n_k > 1$. One can take the leftmost pair of spins in this sequence and move it to the left until joining the left next-neighboring sequence $k - 2$ that is possible because $k - 1$ st sequence is even [transition $A \rightarrow B \rightarrow C$ in Eq. (36)]. Then the leftmost spin pair of $k - 2$ nd sequence (spins 3, 4) moves left to join $k - 4$ th sequence ($C \rightarrow D$). This procedure should be continued until the pair of spins will join the k th sequence from the right [the state D in Eq. (36)]. The final state (D) is formed by the translation of the initial state (A) to the right by two steps. This proves the translational invariance of the associated Krylov subspace and, consequently, eigenstates of the problem.

Using the similar arguments one can give a full description of Krylov subspaces of groups I and II. The states of the group I for N spins and total spin projection S to the z axis for the inverted states (remember that for the group I N must be even and S must be integer) belong to two Krylov subspaces of states made of even sequences with the sequence borders located all either in even or odd positions.

The states and Krylov's subspaces of the group II can be further characterized using the analysis similar to that in Ref. [38] for nonlocal integrals of motion. Such analysis is beyond the scope of this paper targeted to distinguish delocalized, translationally invariant states of groups I and II and almost all localized states of groups III and IV.

Krylov subspaces containing states with both odd- and even-numbered oppositely oriented odd sequences have no translational invariance except for marginal situations including, for instance, Krylov subspaces containing periodic states (e.g., $\{3, 3, 3, 3\}$).

To prove that, consider the closest oppositely oriented odd sequences in odd and even positions. They are separated by the even number of even sequences. These sequences can be removed by means of pair hops from each sequence towards the closest odd sequences with the same direction of spins. Since the spin pair located between two odd sequences cannot hop through them the position of this border is conserved within the Krylov subspace.

The position of the boundary between two odd sequences in that configuration is unique and it cannot be modified by the pair hopping because of the spin-projection conservation to the z axis. Odd sequences are not transparent for pair hopping because pairs move by two steps only. Therefore, adjacent odd sequences confine the spin transport breaking down the translational invariance of corresponding Krylov subspaces. This is not true for the group II states where all odd sequences possess the same spin orientation. Indeed, they can exchange by pairs that can pass through even sequences separating them.

The fixed position of the boundary between neighboring odd sequences in the product state with the minimized number of sequences violates the translational invariance of the Krylov subspace with the only exception of subspaces containing the translationally invariant states composed by self-repeating sets of spins. The simplest translationally invariant states belonging to the group III are given by

self-repeating sequences $\{2p + 1, 2p + 1, \dots, 2p + 1\}$ with any integer p [36].

D. Frozen spins

The majority of states of the system ($\sim 2^N$) belong to the shattered group IV because of the existence of a finite-length frozen-spin groups [35,41] in the large number of spins limit. Indeed, if there exists the frozen-spin group of a finite length it can be characterized by the formation probability P_f per the unit chain length. Consequently, in the large number of spins limit the probability to avoid that group scales approximately as $e^{-P_f N}$ suggesting exponentially small weight of states lacking frozen spins.

How are these frozen groups formed? If a sequence is even and at least one of its neighboring sequences possesses more than one spin, then all spins within that even sequence are mobile since the pair of spins from the neighboring sequence can hop through the sequence under consideration shifting all its spins by two [see, e.g., $A \rightarrow C$ transition in Eq. (36)]. Therefore, an even sequence can belong to the frozen set only if its neighboring sequences contain only one spin.

If an odd sequence has both neighbors containing more than one spin, it is mobile. However, if one of its neighbors has the only one spin, then its edge spin on that side cannot hop until that neighboring sequence changes. Consequently, a single-spin sequence surrounded by two odd sequences (see case A below)

$$\begin{aligned}
 \text{(A)} \quad & \begin{array}{cccccccccccc}
 & 1 & 2 & 3 & 4 & 5 & 6 & 7 & 8 & 9 & 10 & 11 & 12 \\
 & \uparrow & \uparrow & \downarrow & \downarrow & \uparrow & \downarrow & \downarrow & \downarrow & \downarrow & \downarrow & \downarrow & \uparrow \\
 & \uparrow & \downarrow & \uparrow & \downarrow & \uparrow & \downarrow & \downarrow & \downarrow & \downarrow & \downarrow & \downarrow & \uparrow
 \end{array}, \\
 \text{(B)} \quad & \begin{array}{cccccccccccc}
 & \uparrow & \uparrow & \downarrow & \downarrow & \uparrow & \downarrow & \downarrow & \downarrow & \downarrow & \downarrow & \downarrow & \uparrow \\
 & \uparrow & \downarrow & \uparrow & \downarrow & \uparrow & \downarrow & \downarrow & \downarrow & \downarrow & \downarrow & \downarrow & \uparrow \\
 & \uparrow & \downarrow & \uparrow & \downarrow & \uparrow & \downarrow & \downarrow & \downarrow & \downarrow & \downarrow & \downarrow & \uparrow
 \end{array} \quad (37)
 \end{aligned}$$

forms a simplest frozen set $\{\text{odd}, 1, \text{odd}\}$ with three frozen spins at positions (5, 6, 7) shown within the box in the state A in Eq. (37). If the set $\{\text{odd}, 1\}$ is followed by the sequence with an even number of spins, it should have the next sequence containing only a single spin to keep spins being frozen. The fragment $\{\text{even}, 1\}$ can be added an arbitrary number of times [n in Eq. (37), state B] until being terminated by the odd sequence. This is the only way of creating a finite-size frozen set of spins just by construction.

Completely frozen states must have each sequence with more than one spin being surrounded by single-spin sequences (except for the state of all identical spins). Using this definition we determine the number of such states as 1.134×1.7549^N (see Supplemental Material [59], Sec. II B).

E. States possessing odd number of spins

We cannot invert spins in a periodic chain with an odd number of spins since odd positions become even after passing the period as shown below:

$$\begin{aligned}
 \text{(A)} \quad & \downarrow \uparrow \downarrow \downarrow \uparrow \rightarrow (\text{A}_1) \downarrow \downarrow \uparrow \uparrow \downarrow, \\
 \text{(B)} \quad & \begin{array}{cccccc}
 1 & 2 & 3 & 4 & 5 \\
 \downarrow & \downarrow & \downarrow & \uparrow & \uparrow
 \end{array} \rightarrow (\text{B}_1) \begin{array}{cccccc}
 1 & 4 & 5 & 2 & 3 \\
 \downarrow & \uparrow & \uparrow & \downarrow & \downarrow
 \end{array} \rightarrow (\text{B}_2) \begin{array}{ccccc}
 5 & 3 & 1 & 2 & 4 \\
 \uparrow & \downarrow & \downarrow & \downarrow & \uparrow
 \end{array}, \\
 \text{(C)} \quad & \begin{array}{cccccccccc}
 1 & 2 & 3 & 4 & 5 & 6 & 7 & 8 & 9 & 10 \\
 \downarrow & \downarrow & \downarrow & \uparrow & \uparrow & \uparrow & \uparrow & \downarrow & \downarrow & \downarrow
 \end{array} \rightarrow (\text{C}_1) \begin{array}{cccccccccc}
 1 & 4 & 5 & 2 & 3 & 6 & 9 & 10 & 7 & 8 \\
 \downarrow & \uparrow & \uparrow & \downarrow & \downarrow & \downarrow & \downarrow & \uparrow & \uparrow & \downarrow
 \end{array}. \quad (38)
 \end{aligned}$$

In the inverted chain with overturned spins in even positions the state A transforms to the state B. According to the rules for the pair hopping in addition to the pair hopping leading to the state B_1 (the straight chain state A_1) there is the pair hopping through the border to the state B_2 , which is not permitted for the straight state. This problem can be resolved adding the second chain that is the fully inverted copy of the first chain [see the state C in Eq. (38)]. Then the pair hopping should be performed simultaneously for the pair and its copy like it is shown for the transition $C \rightarrow C_1$ where the hopping of the pair of spins 2 and 3 by two steps to the right is accompanied by the hopping of its inverted copy [spins (7, 8)] by two steps to the right. There is only one allowed pair hopping from the state C_1 backwards to the state C. Thus, this double chain with partially inverted spins have hopping of pairs equivalent to dipole moment conserving transitions in the straight spin chain.

Consequently, one can construct the Krylov subspace in double-inverted chain using simultaneous hopping of pairs and their copies shifted by N . Similarly to the previous consideration, a simultaneous existence of odd sequences in even and odd positions breaks down the translational invariance of the Krylov subspace. It turns out that such sequences exist inevitably in any state of $2N$ spins for an odd number of spins N .

Indeed, for an odd total number of spins N at least one sequence containing an odd number of spins must exist. Then, its copy with the opposite spin orientation must exist as well in the copy state. Consequently, we have two sequences with odd numbers of spins occupying odd and even positions (because they are of opposite orientations) that contradict to the requirement for all either odd- or even-numbered sequences to have even numbers of spins, which is the necessary requirement for the translational invariance.

Thus, we show that spin states having an odd number of spins always have confined spin transport and belong either to the group III if all spins are mobile or the group IV if it contains frozen spins [Eq. (37)].

F. Group-averaged imbalances

Here we consider the connection between the groups, defined in Sec. III B, and dynamic properties of states belonging to these groups expressed in terms of experimentally accessible imbalance determined by the evolution of the initial product state [33,66]. The average imbalance for the initial product state a is defined as [33]

$$I_a(t) = \frac{\frac{1}{N} \sum_{k=1}^N \langle S_k^z(t) \rangle \langle S_k^z(0) \rangle - \langle S_{k|*}^z \rangle^2}{1/4 - \langle S_{k|*}^z \rangle^2}, \quad (39)$$

where $\langle S_k^z(0) \rangle$ is the projection of the spin k to the z axis in the state a , $\langle S_k^z(t) \rangle$ is the average projection of this spin to the z axis at time t , and $\langle S_{k|*}^z \rangle$ is the expectation value for the projection of the spin to the z axis in the ergodic system. With this definition the imbalance should approach zero in the ergodic regime at an infinite time and in the thermodynamic limit of an infinite number N of spins [2]. In the localized regime it should remain constant. The convergence of imbalance to its

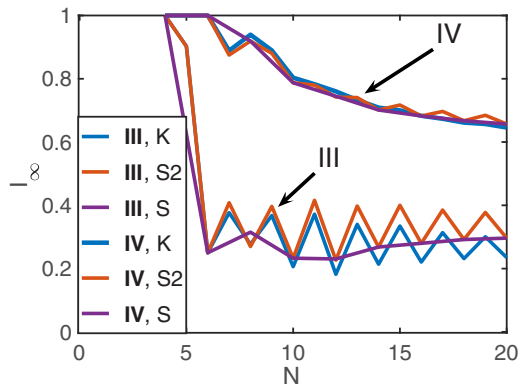


FIG. 3. Comparison of average imbalances for groups III and IV with expectation values evaluated for different subspaces. Letter K means Krylov subspace averaging, letters $S2$ means averaging over subspaces with fixed odd and even sublattice spin projections to the z axis for even number of spins, while S means averaging with the fixed total spin projection to the z axis.

expectation value in the ergodic, delocalized regime has to be exponential as N approaches infinity.

This criterion is used below to distinguish localized and delocalized states. The delocalized regime is not necessarily ergodic [37] and, therefore, we discuss the level statistics in the end of the present section.

How to define correctly expectation value $\langle S_k^z \rangle_*$ in the ergodic regime? In the infinite-temperature limit we assume that all states contributing to the eigenstates should be represented equally in this average. Consequently, spin projections should be averaged over the Krylov subspace defined for each given initial state.

It is straightforward to define average spin projections for Krylov subspaces corresponding to the translationally invariant groups I and II for even numbers of spins. The Hamiltonian (1) conserves the total projections of odd- and even-numbered spins to the z axis ($S_{\text{odd}} = \sum_{k=1}^{N/2} S_{2k-1}^z$ or $S_{\text{even}} = \sum_{k=1}^{N/2} S_{2k}^z$, respectively). Then, the Krylov-subspace-averaged projection of spin k to the z axis is given by $2S_{\text{odd}}/N$ or $2S_{\text{even}}/N$ for odd or even k , respectively, due to the translational invariance of the Krylov subspace with the period 2. We used this definition of expectation values in Eq. (39) for even number of spins and arbitrarily the group of the initial state. For odd number of spins we set the expectation value for the average spin projection equal to its average value $\sum_{k=1}^N S_k^z/N$. With this definition of the spin-projection expectations we evaluated group-averaged imbalances in the infinite-time limit as shown in Fig. 2. The Krylov-subspace-averaged imbalances for groups III and IV are quite close to those evaluated with spin-projection expectation values used in Fig. 2 as illustrated in Fig. 3. Therefore, our definition of expectation values is relevant for all states that are important for the analysis of experimental data. Indeed, it is straightforward to evaluate spin projections using the initial states, while the evaluation of Krylov-subspace-averaged projections can be problematic because of the exponentially large number of states.

The group-averaged imbalances represented in Fig. 2 are obtained averaging imbalances for specific state a over

all states belonging to a certain group. They are given in an infinite-time limit (I_∞) [67]. The infinite-time limit of imbalance is evaluated numerically expanding the time-dependent system wave function over the basis of eigenstates $|\alpha\rangle$ with eigenenergies E_α , obtained using exact diagonalization of the system Hamiltonian, as (remember that we set $\hbar = 1$)

$$|\psi(t)\rangle = \sum_{\alpha} \langle \alpha | a \rangle |\alpha\rangle e^{-iE_\alpha t}. \quad (40)$$

Consequently, the average spin projection at the time t [$\langle S_k^z(t) \rangle$] can be expressed as $\sum_{\alpha, \beta} e^{-i(E_\alpha - E_\beta)t} \langle \alpha | a \rangle \langle a | \beta \rangle \langle \beta | S_k^z | \alpha \rangle$. In the infinite-time limit we leave only terms with $E_\alpha = E_\beta$, while oscillating terms are averaged out. This yields

$$\langle S_k^z(\infty) \rangle = \sum_{\alpha, \beta} \langle \alpha | a \rangle \langle a | \beta \rangle \langle \beta | S_k^z | \alpha \rangle \delta_{E_\alpha, E_\beta}, \quad (41)$$

where the generalized Kronecker symbol $\delta_{E_\alpha, E_\beta}$ is equal to unity for $E_\alpha = E_\beta$ and 0 otherwise.

The infinite-time limit is accessible experimentally using time-averaged imbalance as demonstrated in the Supplemental Material [59], Sec. III.

The dependence of group-average imbalances on the number of spins is consistent with our expectations. The average imbalances approach zero exponentially with increasing N for delocalized states of groups I and II and remains finite for other two groups with increasing N .

The convergence of imbalance to its expectation value in Fig. 2 is exponential in the number of spins N for groups I and II as it is expected for the ergodic behavior. However, the additional analysis of the level statistics (to be reported elsewhere) suggests ergodic behavior only for the states belonging to the group II, that is consistent with earlier expectations for the Bethe ansatz integrable nature of the group I states for the present problem (1). However, the addition of a small amount of quenched disorder should make the system ergodic [68].

The actual imbalance is affected by the Schrieffer-Wolff rotation modifying the definitions of the spin-projection operators compared to the minimalist model, Fig. 3. However, we expect this effect of order of $(J/F)^2$ to be of a minor significance already at $F > 3J$.

IV. DISCUSSION OF THE RECENT EXPERIMENTS [32,33]: HOW TO OBSERVE DELOCALIZATION AT LARGE FIELD GRADIENTS?

Here we discuss the spin systems investigated experimentally in Refs. [32,33] that are similar to those considered in this work. For a large field gradient $F \approx 2.5J$ a substantial localization was observed in these experiments for all probed initial states in contrast with the expected coexistence of localized and delocalized states. In our opinion, this is the consequence of system inhomogeneity due to the open boundaries [32,33] and the lack of some spin-spin next-neighbor interactions in the system, investigated in Ref. [32]. Below we show for both systems that removing inhomogeneity and making them periodic following the receipt of Sec. II B one can observe delocalization of states belonging to the groups I and II at arbitrary large field gradient.

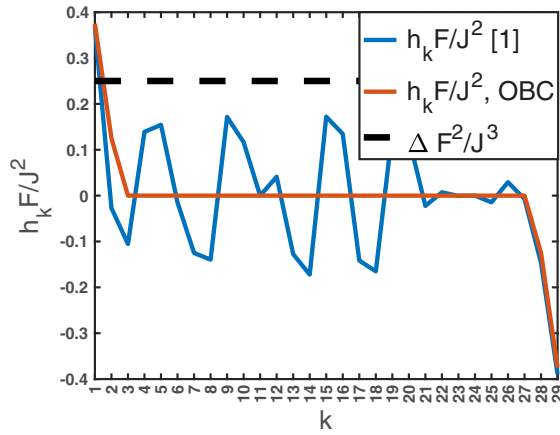


FIG. 4. Longitudinal fields vs the number of spin k generated by means of the Schrieffer-Wolff transformation in the model of Ref. [32] (blue line) and in the OBC model with all identical interactions between nearest- and next-neighbor spins (red line) compared to the four-spin hopping interaction conserving dipole moment (dashed black line).

A. Interacting qubits within the superconducting quantum processor [32]

Two systems of 16 and 29 qubits within the superconducting quantum processor were investigated in Ref. [32]. Both systems can be represented by XY models of interacting spins $\frac{1}{2}$ (qubits) placed into uniformly growing field. For 16 spins only nearest-neighbor interactions were used so the system can be reduced to free fermions [62]. For this system the full Wannier-Stark localization of all states always takes place, so we do not consider it.

Thus, the system of our interest is formed by 29 qubits (spins $\frac{1}{2}$) arranged in a chain with the nearest- and next-neighbor hopping interactions $J_{ij}S_i^+S_j^-$ all defined in Fig. S2.A in the Supplemental Material of Ref. [32] with almost identical interactions J_{ij} for a majority of nearest- and next-neighbor interactions except for several lacking next-neighbor interactions. There is no direct interaction between the ends of the chain, so the OBC regime is realized. Consequently, at large field gradients the effective Hamiltonian of the system contains static longitudinal fields h_k acting on spins, which are generated in the second order of the Schrieffer-Wolff expansion (6) in the form

$$h_k = -\frac{1}{4F} \sum_{l \neq k} \frac{J_{kl}^2}{(k-l)}. \quad (42)$$

These fields are shown in Fig. 4 where they are rescaled by the factor J^2/F and compared with four-spin hopping amplitude Δ [Eq. (1)] rescaled by the factor J^3/F^2 . Their relationship in Fig. 4 corresponds to the case of $J = F$. Even in that case a typical field is comparable with the hopping strength, while for larger field gradient F the ratio of generated fields and the hopping amplitude increases proportionally to F . Consequently, in this limit the full many-body localization should be naturally expected in agreement with the experimental results [32].

However, if we set all neighbor and next-neighbor interactions equal to each other (leaving other interactions equal to

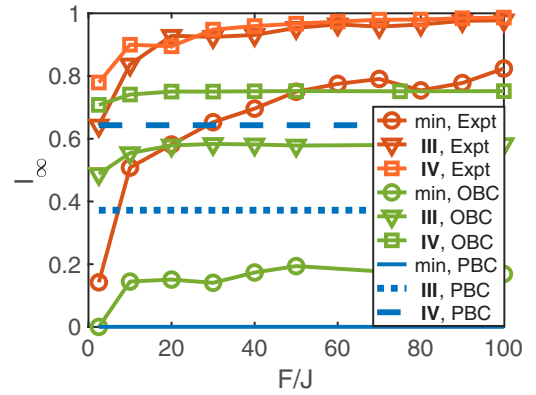


FIG. 5. Average infinite-time imbalances for groups III and IV and minimum imbalances vs a field gradient F . The results are given for the models of Ref. [32] (Expt.), OBC, and PBC minimalist models.

zero as in Ref. [32]), then the field is induced only in the four edge sites of the spin chain, while it is zero in all other sites (see Fig. 4). In this case (referred in Figs. 4 and 5 as the OBC model) delocalization can take place for all spins, except for those at edges, at arbitrarily large field gradient. If in addition the system is made periodic implementing the time-periodic Hamiltonian of Eq. (12), then no longitudinal field exists. In the latter case the states should be separable into localized and delocalized groups in accord with Sec. III.

Here we report the investigation of imbalances in all three models referred as that of Ref. [32], OBC, and PBC within the minimalist models represented by the Schrieffer-Wolff expansion up to the third order in J/F for $F \gg J$. Since the number of spins in Ref. [32] is odd ($N = 29$) the product states can belong only to groups III or IV. We evaluated average imbalances within the infinite-time limit for these groups for all three models choosing initial state randomly and collecting data until the standard deviation of the average imbalance for each group exceeds 0.5%. We also collected minimum imbalances for all considered states to approach most delocalized states. It is natural to expect that the initial state possessing the minimum imbalance belongs to the Krylov subspace with most delocalized states. Average spin projections in the initial product states were used for spin-projection expectation values in the definition of imbalance [Eq. (39)] similarly to Sec. III F for an odd number of spins.

The Monte Carlo estimate of imbalances has been compared with the exact calculations for the system of $N = 20$ spins where it gives quite reasonable estimate both for average and minimum imbalances. This justifies its application to $N = 29$ spins.

Average imbalances for the groups III and IV and minimum imbalances are shown in Fig. 5. The imbalance behavior indicates substantial localization in the model of Ref. [32] with increasing the field gradient F where average and minimum imbalances increase with increasing F approaching the maximum value 1. This is due to longitudinal fields (see Fig. 4) suppressing delocalization stronger at larger F . In OBC and PBC models, imbalances are almost or completely field gradient independent because there are no generated longitudinal fields for the majority of spins (OBC) or all

spins (PBC) in these models. Yet, finite average imbalances suggest substantial localization of states in both models that is consistent with the nature of the groups III and IV.

The minimum imbalance for the model generated using experimental parameters [32] and at the field gradient $F = 2.5J$ is $I_{\min} = 0.1423$. It is realized for the initial state $\uparrow\uparrow\uparrow\downarrow\downarrow\downarrow\uparrow\uparrow\downarrow\downarrow\uparrow\uparrow\downarrow\downarrow\uparrow\downarrow\uparrow\downarrow\uparrow\downarrow\uparrow\downarrow$. The corresponding eigenstates are partially delocalized, yet representing the minority of states since the average imbalance exceeds 0.6 (see Fig. 5). Further increase of the field gradient leads to the increase of the minimum imbalance (e.g., $I_{\min} = 0.5$ for $F = 8J$) indicating the localization of all states due to generated static fields.

The minimum imbalance for the PBC model $I_{\min} = 0.27 \times 10^{-3}$ indicates a substantial delocalization of corresponding states (initial state is $\uparrow\downarrow\uparrow\uparrow\downarrow\downarrow\uparrow\downarrow\uparrow\downarrow\uparrow\downarrow\uparrow\downarrow\uparrow\downarrow$). Thus, delocalization of a minority of states is possible for the group III states where all spins are mobile. The minimum imbalance for the OBC model at large field gradient realized for the initial state $\downarrow\downarrow\downarrow\uparrow\downarrow\uparrow\downarrow\uparrow\downarrow\uparrow\downarrow\uparrow\downarrow\uparrow\downarrow\uparrow\downarrow\uparrow\downarrow\uparrow$ is around 0.15. This estimate is approximately consistent with the minimum imbalance estimate $4/29 \sim 0.14$ for the fully delocalized state where all spins except for the four spins at the chain boundaries suppose to have time averages close to zero. Therefore, there can be a substantial delocalization for some states of the OBC model. For the minimum considered field gradient $F = 2.5J$ the minimum imbalance for that model approaches zero.

Thus, delocalization of some states in the system studied in Ref. [32] can be attained in the large field gradient limit by making the spin-spin interactions between nearest- and next-neighbor spins identical. The delocalization can be further strengthened by means of making the system periodic and using an even number of spins as shown in Fig. 2 for the groups I and II.

Our consideration is limited to the minimalist model. The numerical study of more accurate models for the system of 29 spins is problematic because of the huge number of states involved. Yet, we believe that our results remain valid at least qualitatively according to the analysis of Sec. II C.

B. Trapped ion quantum simulator [33]

Here we examine the chain of $N = 15$ spins with the hopping interaction $J_{ij} = 1/|i - j|^{1.3}$ placed in a uniformly growing field with the gradient F [Eq. (2)]. This model approximately represents interacting cold atoms investigated in Ref. [33]. Another system of 25 atoms was also considered there. However, the latter system is too complicated for our consideration because of the very large Hilbert space (over 10^5 states with the total spin $\frac{1}{2}$ and fixed dipole moment $P = 0$ modulo 25). The consideration was still possible for the system of 29 spins examined earlier (Sec. IV A) because its effective Hamiltonian possesses a smaller Krylov subspace due to a short-range interaction there.

Experimentally investigated systems are characterized by open boundary conditions (OBC). Consequently, similarly to Sec. IV A, there exist static longitudinal fields generated in the second order of perturbation theory [Eq. (6)], as shown in

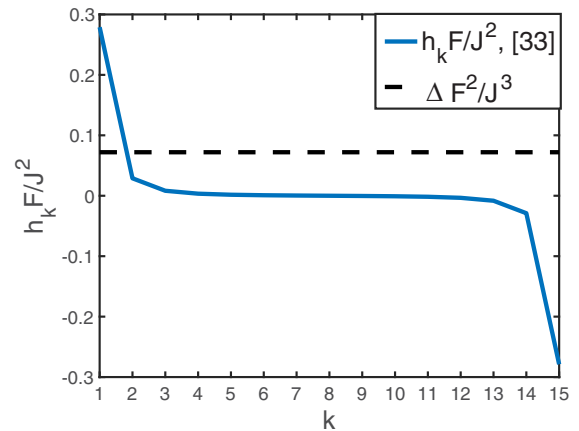


FIG. 6. Longitudinal fields vs the number of spins k generated by means of the Schrieffer-Wolff transformation in the model of Ref. [33] (blue line) compared to the four-spin hopping interaction conserving dipole moment (dashed black line).

Fig. 6 where the fields are rescaled by the factor J^2/F and compared with four-spin hopping amplitude rescaled by the factor J^3/F^2 similarly to that in Fig. 4 in Sec. IV A. In the case of $J = F$ depicted in Fig. 6, only fields acting on the spins at the edges exceed the four-spin hopping amplitude, while for larger field gradient F other fields will be also significant. Eventually in the large field gradient limit $F \rightarrow \infty$ many-body localization of all states should take place in accord with the experimental observations [33] similarly to that for Ref. [32] as it was shown in Sec. IV A. A different behavior is expected for the periodic model lacking longitudinal fields.

To examine the effect of boundary conditions and the relevance of spin-state groups we evaluated imbalances exactly for the OBC [Eq. (2)] and PBC [Eq. (12)] models. We use hopping amplitudes $J_{ij} = J/r_{ij}^{1.3}$ as in Ref. [33] with $r_{ij} = |i - j|$ in the OBC model and $r_{ij} = 2N|\sin[\pi(i - j)/N]|/\pi$ in the PBC model to make it periodic on a circle. The dependence of group-averaged imbalances on the field gradient is investigated for $N = 12$ to examine the relevance and applicability of the groups. We also evaluated imbalances for the maximum field gradient $F = 2.5J$ used experimentally for the system of 15 spins and compare the results with the periodic system of 14 spins at the same field gradient $F = 2.5J$.

The division of states into groups is not formally applicable to the power-law hopping J_{ij} since in the limit of a large field gradient four-spin hopping [Eq. (11)] can involve arbitrary quartets of spins with transitions conserving dipole moments. However, it can be valid approximately because the dominating hopping is still local due to the fast decrease of its amplitude with the interspin distance. For example, the hopping amplitude for the quartet transition $S_i^+ S_{i+1}^- S_{i+3}^- S_{i+4}^+$ of two spin pairs separated by one interatomic distance is less than that for the local quartet $S_i^+ S_{i+1}^- S_{i+2}^- S_{i+3}^+$ by almost a factor of 10 (8.0).

It is not clear whether the power-law hopping within the parent model would lead to the inevitable localization breakdown in the infinite number of spins limit. According to the preliminary analysis, the hopping $1/r^{1.3}$ in the case of the strong field gradient does not inevitably lead to all state

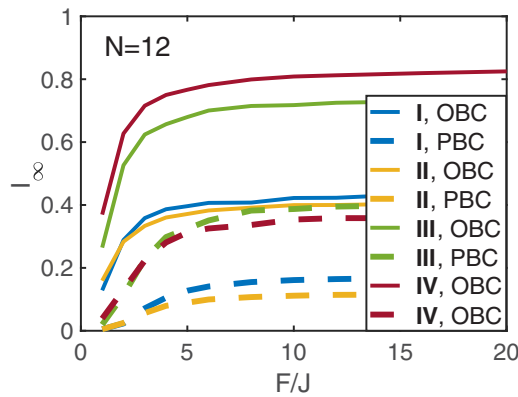


FIG. 7. Group-averaged imbalance for the periodic and open boundary condition realizations of the system of Ref. [33] vs the field gradient for $N = 12$.

delocalization as in the models of Refs. [57,69–73]. Localization can be unstable for interaction decreasing slower with the distance. Particularly, the recent work [74] reports the number of interesting behaviors in the Stark MBL problem in the case of infinite-range distant-independent transverse interactions that await the proper interpretation and experimental verification. It is not clear whether the ergodic spot arguments [75] are applicable to the present problem as well because of the lack of quenched disorder.

To examine the applicability of the group concept to the system of interest we evaluated imbalances for different initial states and averaged them over initial state groups for $N = 12$. The infinite-time limit of group-averaged imbalances is shown in Fig. 7 for the system with open boundary conditions (OBC) corresponding to the experiment and the periodic system for 12 spins. In both cases, imbalances are distinguishable for different groups already for $F > 2J$. This domain includes the experimentally probed field gradients $F \leq 2.5J$. As noticed in Sec. II B the dependence of imbalance on the field gradient saturates at $F \geq 4J$. For the OBC problem imbalance slowly increases with the field gradient due to the localization effect of the longitudinal field induced by the boundaries (see Fig. 6).

The behavior of average imbalances is qualitatively similar to that for the previously considered 29 spins with short-range interactions (see Fig. 5). Initial states of the group IV correspond to larger imbalances compared to the states of the group III in accord with our expectations. For OBC systems the average imbalance increases with increasing the field gradient F towards its maximum value of 1. The minimum imbalance also increases with F , indicating localization of all system states.

For the experimentally relevant OBC model of 15 spins and $F = 2.5J$ the minimum imbalance $I_{\min} = 0.1364$ is found for the initial state $\downarrow\downarrow\uparrow\uparrow\downarrow\downarrow\downarrow\downarrow\uparrow\uparrow\downarrow\downarrow\uparrow\downarrow\uparrow$. The average imbalances for the groups III and IV are given by 0.5221 and 0.6787, respectively. This observation suggests the localization of the majority of states in a sharp contrast with the PBC problem for $N = 14$ and $F = 2.5J$. Group-average imbalances for this problem are given by 0.055, 0.04, 0.088, 0.1877 for the groups I–IV, respectively. Thus, the minimum

imbalance for the OBC problem is comparable to the averaged imbalance for the most localized group IV for the PBC problem.

This observation suggests delocalization of states for the first three groups and localization of most of states belonging to the fourth one. It is consistent with that for the minimalist model (1) except for the group III. However, since there exists nonlocal hopping this observation is approximately consistent with that in the Supplemental Material [59] [Sec. I, Fig. 3(b)]. It was shown there that the addition of the fourth-order nonlocal interaction suppresses localization of states of the group III for a field gradient $F < 25J$ and even numbers of spins. Consequently, the system containing even numbers of interacting spins with periodic boundary conditions is most suitable to investigate coexistence of localization and delocalization.

V. DISCUSSIONS AND CONCLUSIONS

Here we summarize the results of this work and compare them with other work [36–38,41] where the composite blocks (pseudospins, dipoles, defects) were introduced to characterize dipole moment conserving spin dynamics. The results can be divided into three parts discussed separately including the classification of Krylov subspaces for the minimalist model (Sec. V A), understanding spin dynamics in different groups of Krylov subspaces (Sec. V B), and the application of these findings to existing experiments (Sec. V C).

A. Understanding Krylov subspaces

The visually transparent consideration of spin dynamics in the minimalist periodic dipole moment conserving (modulo N) model for the chain of N spins $\frac{1}{2}$ [Eq. (1)] has been proposed using inverted spin chain with all even-numbered spins overturned about the x axis by the angle π . Then the spin transport for even numbers of spins can be represented as hops of pairs of identically oriented spins by two chain periods to the right or to the left. This representation is used to separate all product states and associated Krylov subspaces into four groups based on the parity of identically oriented spin sequences.

1. Groups of states

The inverted chain states belonging to the group I are composed by the only even sequences (see Fig. 1). Corresponding Krylov subspaces are translationally invariant. Consequently, eigenstates are delocalized. Their dynamics is characterized by the Bethe ansatz integrable anisotropic Heisenberg model for the pseudospins $\frac{1}{2}$ created from adjacent spin pairs similarly to Refs. [36,48].

The inverted states belonging to the group II have even number of spins in all sequences of adjacent spins oriented either upwards or downwards, while the oppositely oriented sequences must have at least one sequence with more than one spin. Corresponding Krylov subspaces are translationally invariant. Eigenstates belonging to this group are delocalized and we expect them to be ergodic based on the preliminary analysis of the level statistics.

Several Krylov subspaces composed by specific combinations of pseudospins and dipoles belonging to the group

II and possessing delocalized eigenstates were identified in Ref. [37]. The transport visualization using inverted lattice permitted us to move further and identify all translationally invariant subspaces, thus generalizing the previous work.

The inverted states possessing both upwards and downwards oriented sequences with odd numbers of spins and systems with odd numbers of spins are characterized by nontranslationally invariant Krylov subspaces with marginal exceptions of subspaces containing translationally invariant product states, considered in Ref. [36]. These states can be separated into two groups including the group III of states with all mobile spins and group IV, of states possessing frozen spins. All spin sets containing frozen spins are identified.

2. Numbers of states

The numbers of states belonging to all groups increase exponentially with the numbers of spins N . We evaluated this dependence analytically using the generating function method. The number of states increases with the number of the group. The majority of states belong to the group IV.

3. Integrals of motion

It is possible to identify a number of conserving quantities similarly to Ref. [38] where such quantities were considered for the dipole moment conserving transport in the spin $S = 1$ chain. This includes, for instance, the number of spin sequences within the representative product state containing an odd number of spins or the parity of the numbers of spins at odd sequence boundaries (the leftmost spin is always odd, while the rightmost spin is always even or vice versa). In this work we do not attempt to identify all such integrals of motion concentrating more on the localization problem. Yet, below in Sec. VB we recognize their significance for understanding spin dynamics.

4. Possible extension of the arguments to the spin $S = 1$ case

Visualization of spin dynamics within the inverted lattice permits us to represent it as moving vehicles, composed by pairs of adjacent, identically oriented spins, within the environment of the oppositely oriented spins. Similarly, for the minimalist dipole moment conserving spin-1 problem [35] one can introduce such vehicles made of adjacent spins with opposite projections ± 1 . Then, these vehicles can move freely within the environment of the spins with the zero projection.

It can be shown (we leave the proof to the readers) that with marginal exceptions the product states forming translationally invariant Krylov subspaces must have spins with the projections $S^z = \pm 1$ arranged in the way that each spin with a projection $S^z = \pm 1$ has at least one of the two neighboring spins with $|S^z| = 1$ having the opposite projection $S^z = \mp 1$ (that spin can be separated from the given spin by an arbitrary number of spins with the zero projection). Further extensions of theory to more complicated models can be possibly developed, which is beyond the scope of this work.

B. Localization and delocalization of states in different groups: Connection to the parent model

It is quite natural to expect delocalization of eigenstates belonging to the translationally invariant groups I and II and localization for the states of the group IV possessing the immobile spins. These expectations are fully confirmed by the investigation of the infinite-time imbalances. The study of imbalances also shows the localization of almost all states belonging to the group III lacking translational invariance but with all mobile spins.

The model considered in Refs. [36,37,41] is different from Eq. (1) because it does not include the longitudinal part containing S^z operators. Remember that this part of the Hamiltonian is the outcome of generalized Schrieffer-Wolff expansion of the parent XY model, which makes our model more relevant experimentally. To the best of our knowledge in other systems the strong longitudinal interaction is always unavoidable.

To compare system dynamics in two different models we evaluated average imbalances for all groups of states for the model of Refs. [36,37,41]. It turns out that the imbalances behave nearly identically for all groups except for the group III, where the ergodic behavior is found in contrast to the localization in the model (1), considered in this work.

What is the origin of this difference? In our opinion the longitudinal interaction acts as a quasistatic disorder, localizing spin dynamics. The static nature of disorder can be the consequence of the conserving quantities (cf. Ref. [38]) including the number of odd sequences and positions of their borders that can occupy limited number of places due to the translational invariance breakdown. It is not clear whether this localization survives for group III states in a thermodynamic limit of an infinite system. At least no signature of localization breakdown is seen in Fig. 2 up to $N = 30$.

The localizing effect of the longitudinal interactions should be even stronger in other systems including the fractional quantum Hall problem in the thin-torus limit [36,48–50] and the anisotropic Heisenberg model with nearest-neighbor interactions subjected to a uniformly growing field in a large field gradient limit [41,60,61]. In both limits justifying the transverse interaction in the form of Eq. (1) there exist longitudinal interactions exceeding the transverse interaction by the expansion parameter. This should increase the strength of static disorder and the localization trend. Consequently, the present model is expected to be most delocalized, that justifies its experimental and theoretical considerations.

The concept of the groups of states is extendable at least qualitatively to the parent models with time-periodic Hamiltonians that can be used to realize the minimalist model experimentally for the large field gradient F . It is possible that localization survives there for $F > J$ because of the quasistatic disorder induced by some integrals of motion including, for example, the approximately conserving dipole moment. This expectation is consistent with the recent observation of Stark gauge protection [76], where the disorder-free localization in several quantum gauge theory realizations has been stabilized by the uniformly growing potential in spite of the presence of gauge-breaking interactions.

C. Interpretation of experiments and suggestion of their advancement

The localization observed experimentally in Refs. [32,33] for the large field gradient $F \sim 2.5J$ turns out to be the consequence of the boundaries and lack of certain interactions in Ref. [32]. This issue can be resolved using the periodic spin chain under action of a time-varying Hamiltonian suggested within this work. Then the system becomes translationally invariant and it should show a full diversity of behaviors depending on the group of the initial state.

The initial product states possessing the minimum imbalances are determined for various experimental settings. It can be worth to probe these substantially delocalized regimes experimentally.

ACKNOWLEDGMENTS

A.B. acknowledges the support by Carrol Lavin Bernick Foundation Research Grant (2020–2021), NSF Grant No. CHE-2201027, and LINK Program of the NSF and Louisiana Board of Regents, Award No. LEQSF-EPS(2022)-LINK-136.

-
- [1] J. M. Deutsch, Quantum statistical mechanics in a closed system, *Phys. Rev. A* **43**, 2046 (1991).
- [2] M. Srednicki, Chaos and quantum thermalization, *Phys. Rev. E* **50**, 888 (1994).
- [3] N. Y. Yao, C. R. Laumann, J. I. Cirac, M. D. Lukin, and J. E. Moore, Quasi-Many-Body Localization in Translation-Invariant Systems, *Phys. Rev. Lett.* **117**, 240601 (2016).
- [4] D. Pekker, G. Refael, E. Altman, E. Demler, and V. Oganesyan, Hilbert-Glass Transition: New Universality of Temperature-Tuned Many-Body Dynamical Quantum Criticality, *Phys. Rev. X* **4**, 011052 (2014).
- [5] Y. Bahri, R. Vosk, E. Altman, and A. Vishwanath, Localization and topology protected quantum coherence at the edge of hot matter, *Nat. Commun.* **6**, 7341 (2015).
- [6] A. Chandran, V. Khemani, C. R. Laumann, and S. L. Sondhi, Many-body localization and symmetry-protected topological order, *Phys. Rev. B* **89**, 144201 (2014).
- [7] I. V. Gornyi, A. D. Mirlin, and D. G. Polyakov, Interacting Electrons in Disordered Wires: Anderson Localization and Low- t Transport, *Phys. Rev. Lett.* **95**, 206603 (2005).
- [8] D. M. Basko, I. L. Aleiner, and B. L. Altshuler, Metal-insulator transition in a weakly interacting many-electron system with localized single-particle states, *Ann. Phys.* **321**, 1126 (2006).
- [9] V. Oganesyan and D. A. Huse, Localization of interacting fermions at high temperature, *Phys. Rev. B* **75**, 155111 (2007).
- [10] J. Z. Imbrie, On many-body localization for quantum spin chains, *J. Stat. Phys.* **163**, 998 (2016).
- [11] P. W. Anderson, Absence of diffusion in certain random lattices, *Phys. Rev.* **109**, 1492 (1958).
- [12] L. Fleishman and P. W. Anderson, Interactions and the anderson transition, *Phys. Rev. B* **21**, 2366 (1980).
- [13] Yu. Kagan and L. A. Maksimov, Localization in a system of interacting particles diffusing in a regular crystal, *Zh. Eksp. Teor. Fiz.* **87**, 348 (1984) [*Sov. Phys.–JETP* **60**, 201 (1984)].
- [14] V. A. Mikheev, V. A. Maidanov, and N. P. Mikhin, Localization and quantum diffusion of He³ atoms stimulated by phonons in He⁴ crystals, *Solid State Commun.* **48**, 361 (1983).
- [15] Yu. Kagan and L. A. Maksimov, Effect of interparticle interaction on localization in a nonideal crystal with a narrow band, *Zh. Eksp. Teor. Fiz.* **88**, 992 (1985) [*Sov. Phys.–JETP* **61**, 583 (1985)].
- [16] A. L. Burin, K. N. Kontor, and L. A. Maksimov, Localization and delocalization in the paramagnetic phase of the transverse ising model, *Theor. Math. Phys.* **85**, 1223 (1990).
- [17] D. E. Logan and P. G. Wolynes, Ab initio study of electronic coupling in the aqueous Fe²⁺-Fe³⁺ electron exchange process, *J. Chem. Phys.* **78**, 4086 (1983).
- [18] D. M. Leitner and P. G. Wolynes, Quantization of the Stochastic Pump Model of Arnold Diffusion, *Phys. Rev. Lett.* **79**, 55 (1997).
- [19] B. Georgeot and D. L. Shepelyansky, Integrability and Quantum Chaos in Spin Glass Shards, *Phys. Rev. Lett.* **81**, 5129 (1998).
- [20] G. Carleo, F. Becca, M. Schiró, and M. Fabrizio, Localization and glassy dynamics of many-body quantum systems, *Sci. Rep.* **2**, 243 (2012).
- [21] W. De Roeck and F. Huveneers, Scenario for delocalization in translation-invariant systems, *Phys. Rev. B* **90**, 165137 (2014).
- [22] M. Schiulaz, A. Silva, and M. Müller, Dynamics in many-body localized quantum systems without disorder, *Phys. Rev. B* **91**, 184202 (2015).
- [23] Z. Papić, E. M. Stoudenmire, and D. A. Abanin, Many-body localization in disorder-free systems: The importance of finite-size constraints, *Ann. Phys.* **362**, 714 (2015).
- [24] A. A. Michailidis, M. Žnidarič, M. Medvedyeva, D. A. Abanin, T. Prosen, and Z. Papić, Slow dynamics in translation-invariant quantum lattice models, *Phys. Rev. B* **97**, 104307 (2018).
- [25] M. Brenes, M. Dalmonte, M. Heyl, and A. Scardicchio, Many-Body Localization Dynamics from Gauge Invariance, *Phys. Rev. Lett.* **120**, 030601 (2018).
- [26] M. Serbyn, D. A. Abanin, and Z. Papić, Quantum many-body scars and weak breaking of ergodicity, *Nat. Phys.* **17**, 675 (2021).
- [27] A. Smith, J. Knolle, D. L. Kovrizhin, and R. Moessner, Disorder-Free Localization, *Phys. Rev. Lett.* **118**, 266601 (2017).
- [28] A. Smith, J. Knolle, R. Moessner, and D. L. Kovrizhin, Absence of Ergodicity without Quenched Disorder: From Quantum Disentangled Liquids to Many-Body Localization, *Phys. Rev. Lett.* **119**, 176601 (2017).
- [29] E. van Nieuwenburg, Y. Baum, and G. Refael, From Bloch oscillations to many-body localization in clean interacting systems, *Proc. Natl. Acad. Sci. USA* **116**, 9269 (2019).
- [30] M. Schulz, C. A. Hooley, R. Moessner, and F. Pollmann, Stark Many-Body Localization, *Phys. Rev. Lett.* **122**, 040606 (2019).
- [31] E. Guardado-Sanchez, A. Morningstar, B. M. Spar, P. T. Brown, D. A. Huse, and W. S. Bakr, Subdiffusion and Heat Transport in a Tilted Two-Dimensional Fermi-Hubbard System, *Phys. Rev. X* **10**, 011042 (2020).

- [32] Q. Guo, C. Cheng, H. Li, S. Xu, P. Zhang, Z. Wang, C. Song, W. Liu, W. Ren, H. Dong, R. Mondaini, and H. Wang, Stark Many-Body Localization on a Superconducting Quantum Processor, *Phys. Rev. Lett.* **127**, 240502 (2021).
- [33] W. Morong, F. Liu, P. Becker, K. S. Collins, L. Feng, A. Kyprianidis, G. Pagano, T. You, A. V. Gorshkov, and C. Monroe, Observation of Stark many-body localization without disorder, *Nature (London)* **599**, 393 (2021).
- [34] A. Smith, J. Knolle, R. Moessner, and D. L. Kovrizhin, Dynamical localization in \mathbb{Z}_2 lattice gauge theories, *Phys. Rev. B* **97**, 245137 (2018).
- [35] P. Sala, T. Rakovszky, R. Verresen, M. Knap, and F. Pollmann, Ergodicity Breaking Arising from Hilbert Space Fragmentation in Dipole-Conserving Hamiltonians, *Phys. Rev. X* **10**, 011047 (2020).
- [36] S. Moudgalya, B. A. Bernevig, and N. Regnault, Quantum many-body scars in a Landau level on a thin torus, *Phys. Rev. B* **102**, 195150 (2020).
- [37] S. Moudgalya, A. Prem, R. Nandkishore, N. Regnault, and B. A. Bernevig, *Thermalization and its Absence within Krylov Subspaces of a Constrained Hamiltonian*, (World Scientific, Singapore, 2020), pp. 147–209.
- [38] T. Rakovszky, P. Sala, R. Verresen, M. Knap, and F. Pollmann, Statistical localization: From strong fragmentation to strong edge modes, *Phys. Rev. B* **101**, 125126 (2020).
- [39] V. Khemani, M. Hermele, and R. Nandkishore, Localization from Hilbert space shattering: From theory to physical realizations, *Phys. Rev. B* **101**, 174204 (2020).
- [40] A. Morningstar, V. Khemani, and D. A. Huse, Kinetically constrained freezing transition in a dipole-conserving system, *Phys. Rev. B* **101**, 214205 (2020).
- [41] L. Herviou, J. H. Bardarson, and N. Regnault, Many-body localization in a fragmented Hilbert space, *Phys. Rev. B* **103**, 134207 (2021).
- [42] J. Richter and A. Pal, Anomalous hydrodynamics in a class of scarred frustration-free Hamiltonians, *Phys. Rev. Research* **4**, L012003 (2022).
- [43] J. Feldmeier, P. Sala, G. De Tomasi, F. Pollmann, and M. Knap, Anomalous Diffusion in Dipole- and Higher-Moment-Conserving Systems, *Phys. Rev. Lett.* **125**, 245303 (2020).
- [44] I. García-Mata and D. L. Shepelyansky, Nonlinear delocalization on disordered stark ladder, *Eur. Phys. J. B* **71**, 121 (2009).
- [45] J. Feldmeier and M. Knap, Critically Slow Operator Dynamics in Constrained Many-Body Systems, *Phys. Rev. Lett.* **127**, 235301 (2021).
- [46] E. V. H. Doggen, I. V. Gornyi, and D. G. Polyakov, Stark many-body localization: Evidence for Hilbert-space shattering, *Phys. Rev. B* **103**, L100202 (2021).
- [47] T. Chanda, R. Yao, and J. Zakrzewski, Coexistence of localized and extended phases: Many-body localization in a harmonic trap, *Phys. Rev. Research* **2**, 032039(R) (2020).
- [48] E. J. Bergholtz and A. Karlhede, Half-Filled Lowest Landau Level on a Thin Torus, *Phys. Rev. Lett.* **94**, 026802 (2005).
- [49] A. Seidel, H. Fu, D.-H. Lee, J. M. Leinaas, and J. Moore, Incompressible Quantum Liquids and New Conservation Laws, *Phys. Rev. Lett.* **95**, 266405 (2005).
- [50] Z.-Y. Wang, S. Takayoshi, and M. Nakamura, Spin-chain description of fractional quantum Hall states in the jain series, *Phys. Rev. B* **86**, 155104 (2012).
- [51] S. Scherg, T. Kohlert, P. Sala, F. Pollmann, B. Hebbes Madhusudhana, I. Bloch, and M. Aidelsburger, Observing non-ergodicity due to kinetic constraints in tilted Fermi-Hubbard chains, *Nat. Commun.* **12**, 4490 (2021).
- [52] C. J. Turner, A. A. Michailidis, D. A. Abanin, M. Serbyn, and Z. Papić, Weak ergodicity breaking from quantum many-body scars, *Nat. Phys.* **14**, 745 (2018).
- [53] S. Pai, M. Pretko, and R. M. Nandkishore, Localization in Fractonic Random Circuits, *Phys. Rev. X* **9**, 021003 (2019).
- [54] M. Schreiber, S. S. Hodgman, P. Bordia, H. P. Lüschen, M. H. Fischer, R. Vosk, E. Altman, U. Schneider, and I. Bloch, Observation of many-body localization of interacting fermions in a quasirandom optical lattice, *Science* **349**, 842 (2015).
- [55] R. S. Strichartz, The Campbell-Baker-Hausdorff-Dynkin formula and solutions of differential equations, *J. Funct. Anal.* **72**, 320 (1987).
- [56] R. Achilles and A. Bonfiglioli, The early proofs of the theorem of Campbell, Baker, Hausdorff, and Dynkin, *Archive History Exact Sci.* **66**, 295 (2012).
- [57] A. L. Burin, Localization in a random xy model with long-range interactions: Intermediate case between single-particle and many-body problems, *Phys. Rev. B* **92**, 104428 (2015).
- [58] A. O. Maksymov and A. L. Burin, Many-body localization in spin chains with the long-range transverse interactions: Scaling of critical disorder with the system size, *Phys. Rev. B* **101**, 024201 (2020).
- [59] See Supplemental Material at <http://link.aps.org/supplemental/10.1103/PhysRevB.105.184206> for complementary derivations and analysis.
- [60] E. Wybo, M. Knap, and F. Pollmann, Dynamics of negativity of a Wannier-Stark many-body localized system coupled to a bath, *Phys. Status Solidi* **259**, 2100161 (2022).
- [61] S. R. Taylor, M. Schulz, F. Pollmann, and R. Moessner, Experimental probes of stark many-body localization, *Phys. Rev. B* **102**, 054206 (2020).
- [62] P. Jordan and E. Wigner, Über das Paulische Äquivalenzverbot, *Z. Phys.* **47**, 42 (1928).
- [63] J. R. Schrieffer and P. A. Wolff, Relation between the Anderson and Kondo Hamiltonians, *Phys. Rev.* **149**, 491 (1966).
- [64] S. Biagi, A. Bonfiglioli, and M. Matone, On the baker-campbell-hausdorff theorem: Non-convergence and prolongation issues, *Linear and Multilinear Algebra* **68**, 1310 (2020).
- [65] D. A. Huse, R. Nandkishore, F. Pietracaprina, V. Ros, and A. Scardicchio, Localized systems coupled to small baths: From anderson to zeno, *Phys. Rev. B* **92**, 014203 (2015).
- [66] H. P. Lüschen, P. Bordia, S. S. Hodgman, M. Schreiber, S. Sarkar, A. J. Daley, M. H. Fischer, E. Altman, I. Bloch, and U. Schneider, Signatures of Many-Body Localization in a Controlled Open Quantum System, *Phys. Rev. X* **7**, 011034 (2017).
- [67] V. L. Berezinskii and L. P. Gor'kov, On the theory of electrons localized in the field of defects, *Zh. Eksp. Teor. Fiz.* **77**, 2498 (1979) [*Sov. Phys.-JETP* **50**, 1209 (1979)].
- [68] K. Kudo and T. Deguchi, Level statistics of XXZ spin chains with a random magnetic field, *Phys. Rev. B* **69**, 132404 (2004).
- [69] A. L. Burin, D. Natelson, D. D. Osheroff, and Y. Kagan, Interactions between tunneling defects in amorphous solids, in *Tunneling Systems in Amorphous and Crystalline Solids*, edited by P. Esquinazi (Springer, Berlin, Heidelberg, 1998), pp. 223–315.

- [70] A. L. Burin, Yu. Kagan, L. A. Maksimov, and I. Ya. Polishchuk, Dephasing Rate in Dielectric Glasses at Ultralow Temperatures, *Phys. Rev. Lett.* **80**, 2945 (1998).
- [71] A. L. Burin, Energy delocalization in strongly disordered systems induced by the long-range many-body interaction, [arXiv:cond-mat/0611387](https://arxiv.org/abs/cond-mat/0611387).
- [72] M. Serbyn, M. Knap, S. Gopalakrishnan, Z. Papic, N. Y. Yao, C. R. Laumann, D. A. Abanin, M. D. Lukin, and E. A. Demler, Interferometric Probes of Many-Body Localization, *Phys. Rev. Lett.* **113**, 147204 (2014).
- [73] A. L. Burin, Many-body delocalization in a strongly disordered system with long-range interactions: Finite-size scaling, *Phys. Rev. B* **91**, 094202 (2015).
- [74] Y.-Y. Wang, Z.-H. Sun, and H. Fan, Stark many-body localization transitions in superconducting circuits, *Phys. Rev. B* **104**, 205122 (2021).
- [75] F. Huveneers, Classical and quantum systems: Transport due to rare events, *Ann. Phys.* **529**, 1600384 (2017).
- [76] H. Lang, P. Hauke, J. Knolle, F. Grusdt, and J. C. Halimeh, Disorder-free localization with Stark gauge protection, [arXiv:2203.01338](https://arxiv.org/abs/2203.01338).